Applied Food Research 3 (2023) 100246

Contents lists available at ScienceDirect

Applied Food Research

journal homepage: www.elsevier.com/locate/afres

Spectroscopic techniques for elucidation of structural changes in temperate cowpea cultivars under germination: A useful tool for quality determination and industrial application

Sajad Ahmad Sofi[a], Khalid Muzaffar[a], Asmat Farooq[b], Shafiya Rafiq[a], Darakshan Majid[a], Hilal Ahmad Makroo[a], Shabir Ahmad Mir[c], Amin Mousavi Khaneghah[d,*], Francisco J. Barba[e,*], B.N. Dar[a,*]

[a] Department of Food Technology, Islamic University of Science and Technology Kashmir, 192122, India
[b] Division of Biochemistry, Sher-e-Kashmir University of Agricultural Science and Technology –Chatha, Jammu 190025, India
[c] Department of Food Science and Technology, Govt. Degree College for Woman, Srinagar 190001, India
[d] Department of Fruit and Vegetable Product Technology, Prof. Wacław Dąbrowski Institute of Agricultural and Food Biotechnology State Research Institute, 36 Rakowiecka St., 02-532, Warsaw, Poland
[e] Department of Preventive Medicine and Public Health, Food Science, Toxicology and Forensic Medicine, Faculty of Pharmacy, Universitat de València, Avda. Vicent Andrés Estellés, s/n 46100 Burjassot, València, Spain

ARTICLE INFO

Keywords:
Cowpea
Fluorescence
Germination
Protein Structure
Spectroscopy

ABSTRACT

The present study investigated the molecular changes induced by germination in cowpea cultivars by spectroscopic techniques. The ATR FT-IR, Intrinsic fluorescence, and UV spectroscopic techniques revealed that germination shows alteration in cowpea cultivars. The ATR-FTIR showed slight differences in band intensities corresponding to carbohydrates, lipids, and protein regions at 700 to 4000 cm^{-1} wavenumbers. Starch order structure understanding their functionality showed a reduction of short-range ordered structures in Black cowpea flour and long ordered starch fraction in White cowpea flour under germination. The study quantified the degree of ordered starch and their alteration in amorphous/crystallinity nature concerning germination and cowpea cultivars. The secondary structures revealed a reduction of β-sheets and α-helix content, representing decreased ordered protein structures and their shifting into random coils and turn structures. The germinated flours showed decreased fluorescence intensities with the shift from 347 to 348, reflecting the redshifts due to decreased concentrations of fluorescent compounds during germination in cowpea flour. UV spectrum revealed a similar spectrum with an increase in absorption of cowpea flour under germination. The electrophoresis showed variations in the intensities of high (25 to 225 kDa) and low (19 to 10 kDa) molecular weight proteins in germinated cowpea cultivars than the native one. Overall, this study demonstrated the potential of ATR-FTIR, fluorescence and UV-based spectroscopy as non-destructive techniques to assess the alteration of pulses at the molecular level and structural changes under the germination process.

1. Introduction

Cowpea (*Vigna unguiculata*) edible pulse grain belongs to the Fabaceae family. The cowpea shows geographical origin in Africa and is consumed and grown widely in different areas such as Africa, the USA, and Asia (Appiah, Asibuo, & Kumah, 2011). The worldwide production of cowpea is reported as 6.5 million metric tons annually, with Nigeria producing more than 80%. The USA, Peru, Serbia, Sri Lanka, China, and India are the top cowpea producers globally (Horn & Shimelis, 2020). Nutritional cowpea contains carbohydrates (50–60%), proteins (23–32%), fat (1%), and other health-promoting ingredients such as dietary fiber, polyphenols, minerals, and vitamins (Jayathilake et al., 2018). Cowpea is a nutrient-dense legume rich in proteins with content greater than cereals and an alternate source of animal proteins for vegetarians and people who cannot afford it. The cowpea seeds showed varied diversity based on their color, size, pod size, and geographical distributions. The presence of nutritional and functional ingredients in cowpea flour enhances its usage in developing health-based food (Adjei-Fremah et al., 2019).

Various processing methods of cowpea were used to enhance their techno-functional properties. Germination, fermentation, dehulling, soaking, roasting, cooking, and autoclaving-based methods have been

* Corresponding authors.
E-mail addresses: amin.mousavi@ibprs.pl, mousavi.amin@gmail.com (A. Mousavi Khaneghah), francisco.barba@uv.es (F.J. Barba), darnabi@gmail.com (B.N. Dar).

https://doi.org/10.1016/j.afres.2022.100246
Received 9 August 2022; Received in revised form 10 November 2022; Accepted 7 December 2022
Available online 9 December 2022

used to enhance their nutritional profile, reduce anti-nutritional factors, and suitability for developing functional food (Domínguez-Arispuro et al., 2018; Madodé et al., 2013). Germination is a low-cost technology by induction of biochemical changes and structural changes, generating new components and decreasing the concentration of antinutritional factors (Mir et al., 2021). Germinated pulses with health benefits are considered one of the functional ingredients with improved nutrient compositions, better organoleptic qualities, and the development of nutraceutical foods (Ouazib, Dura, Zaidi, & Rosell, 2016). Germination process increased the protein content of cowpea flour and their digestibility, phytochemicals, antioxidants, vitamin C, and bioactive components and decreased antnutritional factors (phytic acids, trypsin inhibtors, lectins) to produce functional food ingredients with health benefits (Doblado, Frías, & Vidal-Valverde, 2007; De Souza Rocha, Hernandez, Chang, & De Mejía, 2014).

Fourier transform, the infrared type of spectroscopy, is a simple and non-destructive technique to analyze the bond vibrations to detect functional groups and the alteration in the molecular structures (Cocchi et al., 2004). FTIR provides information in the form of qualitative and quantitative manner to determine the molecular alteration in the different forms of the sample (Ferreira, Barros, Coimbra, & Delgadillo, 2001). The FTIR reveals information in the form of peak position, intensity, and shape for revealing the bond and structure of chemical substances. FTIR is used for prediction of compositional analysis, starch structures, and amorphous crystalline fractions (Barron, Parker, Mills, Rouau, & Wilson, 2005; Sevenou, Hill, Farhat, & Mitchell, 2002; Prates, Lei, Refat, Zhang, & Yu, 2018; Holse, Larsen, Hansen, & Engelsen, 2011; Hell, Prückler, Danner, Henniges, Apprich, Rosenau, & Böhmdorfer, 2016; Ferreira, Pallone, & Poppi, 2015; Zhou et al., 2022; Zhu et al., 2022; Hou et al., 2022). The structural proteins in pulses grains undergo conformational changes upon different processing, and their low stability hindered their investigation (Carbonaro & Nucara, 2007). The FTIR vibrational technique is one of the alternate methods for studying protein secondary structures due to the contribution of the amide I band arising due to the C=O peptide bond stretching vibrations (Carbonaro, Maselli, Dore, & Nucara, 2008). The a-helix, b-sheet, turns, and coils-based secondary structure depends on their determination of the vibrational energy associated with the peptide carboxyl group and the assignment of the amide I band spectral components. Several reports on using the FTIR technique to study the protein secondary structures in pulses ((De la Rosa-Millán, Orona-Padilla, Flores-Moreno, & Serna-Saldívar, 2018; Chávez-Murillo, Veyna-Torres, Cavazos-Tamez, de la Rosa-Millán, & Serna-Saldívar, 2018; Shevkani, Singh, Chen, Kaur, & Yu, 2019; Preethi, Moses, & Anandharamakrishnan, 2021). Fluorescence spectroscopy is also a powerful tool to characterize food materials by considering fluorescent molecules as fingerprint substances. Excitation and emission wavelengths were used to analyze fluorescence intensities (Lenhardt, Bro, Zeković, Dramićanin, & Dramićanin, 2015). The research aims to study the effects of germination on temperate cowpea cultivars at the molecular level using spectroscopy techniques.

2. Materials and methods

2.1. Materials

The temperate cowpea cultivars (Black and White) were procured from a local market in Awantipora, Jammu & Kashmir, India. The cow pea cultivars were sowed during month of march 2022, harvested during end of June 2022 and procured from market during month of July 2022. The cowpea cultivars were sorted for unwanted grains, cleaned, dried at 40°C for 4 h and stored at 5°C in a laminated pouches until further use. The ATR-FTIR, Fluorescence and Ultraviolet Spectrum analysis were carried out in Advance Food Analysis Laboratory, Department of Food technology-IUST-Awantipora.

2.2. Germination process

Cowpea seeds with geometric diameters of 4.80 mm for white and 5.32 mm for black cultivars were soaked for 12 h at ambient temperature, and seeds were then placed in the seed germinator (GA-240A, Green Tech, Ambala, India) at optimized conditions (85 % relative humidity and 35°C temperature for 50 h). The germinated seeds were dehusked manually. The dehusked seeds were freeze-dried (Laboman, India), ground into fine flour with particle size of 150 μm using a laboratory mill (IKA- Laboratory Mill), and stored in a refrigerator until used.

2.3. ATR-FTIR spectroscopy

The data of molecular spectral for cowpea flour cultivars were collected from Perkin Elmer ATR-FTIR (Spectrum 1, Perkin Elmer, Norwalk, USA) with attached spectrum software (ver.5.3.0), and the data collected were corrected using air background. The spectral data were recorded with a wavenumber ranging from 4000 to 700 cm^{-1} at 4 cm^{-1} of spectral resolution and 25 scans. The FTIR spectral bands were normalized and smoothed using Origin 2019b software to demonstrate 3700 to 3050 cm^{-1} bands concerning the Amide A band, 3050 to 2800 cm^{-1} for lipid and protein ratios, and 1800 to 1000 cm^{-1} for determination of fingerprint region in terms of absorbance. The starch crystalline and amorphous structures in cowpea under germination were studied by calculation of absorbance at 995 cm^{-1}, 1022 cm^{-1}, and 1047 cm^{-1} IR regions, and their ratios at 1022/995 cm^{-1} and 1047/1022 cm^{-1} were studied for determination of starch short-range ordered structures of cowpea flour samples (Wang, Sun, Wang, Wang, & Copeland, 2016). The amide I band from 1600 to 1700 cm^{-1} represents the secondary structures (β-sheet, random coils, α-helix, and β-turns) that were deconvoluted and fitted to Gaussian fixed-band model using peak deconvolution software (Origin 2019b software) fitted to Gaussian fixed-band model for determination of peak center's assigned to protein secondary structures. Iteration was processed until a satisfactory fit for the bands was obtained. The percentage areas for specific bands of protein secondary structures in the amide I region were calculated from the final fit with converged correlation (R^2) at 0.999 (Sofi, Singh, Muzaffar, & Dar, 2021).

2.4. Fluorescence spectrum analysis

"Fluorescence spectrum was analyzed using Fluorescence Spectrometer (RF 6000-Shimadzu) at 347 nm for excitation wavelength and emission wavelength (330–365 nm) for fluorescence analysis. The slits were set for excitation and emission wavelength at 5.0 nm with a scanning speed of 240 nm min^{-1} (Wang et al., 2020).

2.5. Ultraviolet spectrum analysis

The supernatant of cowpea sample solution of 0.2 mg ml^{-1} by centrifugation at 4000 rpm for 10 min was scanned at 190–500 nm, a scanning rate of 100 nm min−1, and a scanning number of 3 times using an Ultraviolet-visible spectrophotometer (L1600300-Perkin Elmer) against a blank solution of de-dissolved solution (Wang et al., 2020).

2.6. SDS-PAGE

Electrophoresis of cowpea samples was determined as per the standard method of Laemmli (1970). The freeze-dried sample (50 mg) was dissolved in Laemmli sample buffer, and then the sample solution was incubated at 50°C for 90 minutes, heated for 5 min, and centrifuged at 10,000 × g for 1 min. The supernatant of 10 μL was loaded onto the gels (12% separating and 4% stacking gel) using a molecular ladder (10 to 225 KDa) from Promega V849A. The sample gels were stained using Coomassie brilliant blue R250 and then destained using 20% methanol

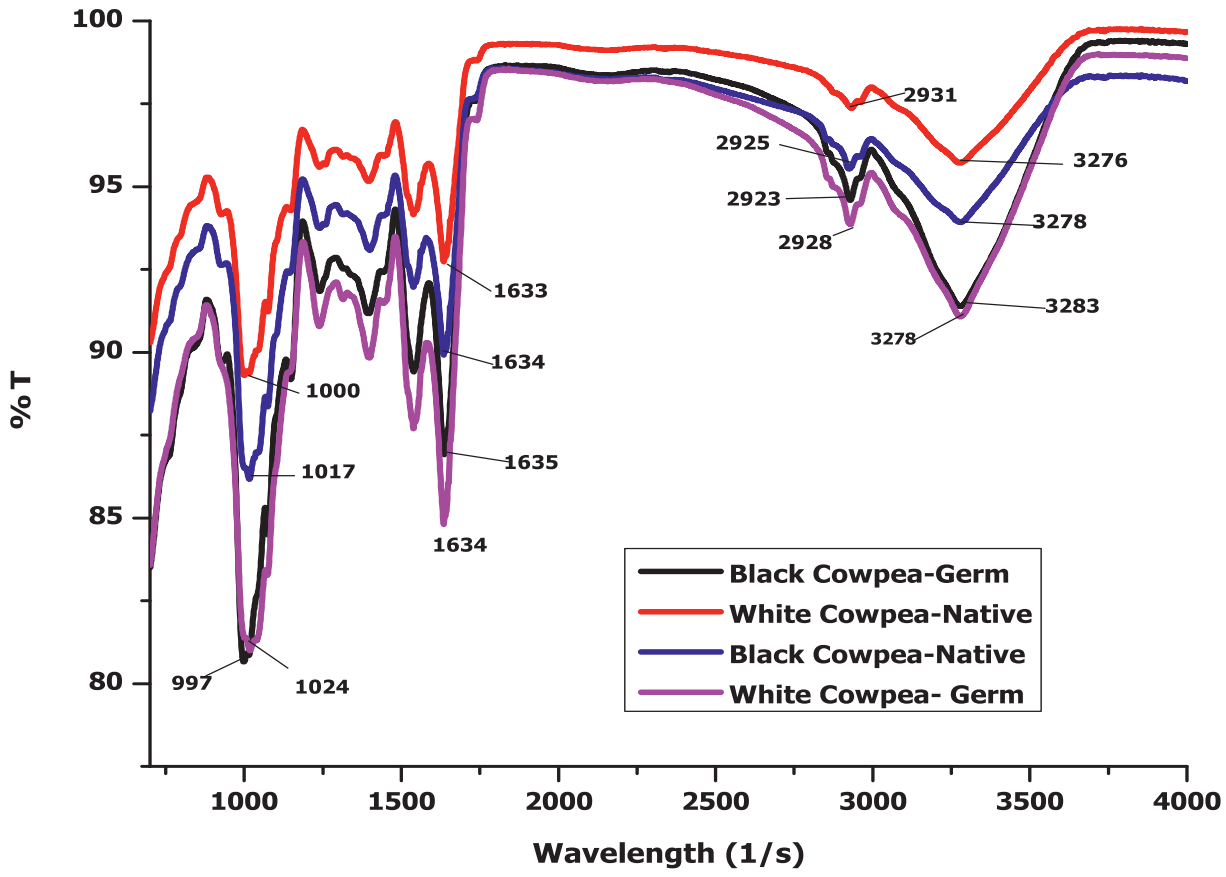

Fig. 1. Representative FT-IR Spectrum of native and germinate Cowpea Flour cultivars.

and 20% glacial acetic acid. The molecular weight and their relative migration (Rf) of sample gels were determined using Gel Molecular Weight Analyzer v1.30.

2.7. Statistical analysis

The experimental results were represented by the mean and standard deviation of three replications. Statistical significance was determined using one-way ANOVA followed by Duncan's mutiple range test at the level of 5 % using software (SPSS 18).

3. Result and discussion

3.1. FTIR-spectroscopy of cowpea flour

FTIR-Spectroscopy was used to analyze the molecular differences and alteration in structural and functional groups in cowpea cultivars under germination. The spectra of native and germinative cowpea flour cultivars (Fig. 1) showed slight differences in bands corresponding to carbohydrates, lipids, and protein zones in the intensity bands from 700 to 4000 cm-^{1} wavelengths. The spectra of native and germinated cowpea flour revealed a decrease in the transmittance of corresponding peaks and an increase in absorbance compared to native. The decreased intensity in germinated cowpea cultivars might be due to the depolymerization of proteins and starch during germination (De la Rosa-Millán, Orona-Padilla, Flores-Moreno, & Serna-Saldívar, 2018). The cowpea from the black and white cultivar showed peak shift in 3700 to 3050 cm^{-1}, 3050 to 2800 cm$^{-1,}$ and 1800 to 1000 cm^{-1} regions of FTIR spectra in the case of germinated cowpea flour, representing conformational changes due to germination process (Kong, & Yu, 2007). The 3700 to 3050 cm^{-1} represents the O-H and N-H group stretching vibrations from polysaccharides, proteins, and lipids (Medhe, Kamble, Kettawan, Monboonpitak & Kettawan, 2022) showing major peaks of 3276 and 3278 cm^{-1} for White and Black native cowpea flour, which showed a small peak shift of 3278 and 3283 cm^{-1}. Fig. 2 represents the spectra of 3700 to 3050 cm^{-1} frequency normalized concerning the Amide A band. The strong band at 3275 cm^{-1} is related to N-H and O-H stretching vibrations of proteins (Vatansever, Ohm, Simsek, & Hall, 2022) showing significant differences between the cowpea cultivars and germinated ones. The absorbance of the 3275 cm^{-1} band was increased from 0.019 to 0.040 in White cowpea and 0.027 to 0.039 in Black cowpea cultivars due to germination, showing an alteration of proteins in cowpea flour during the germination process. The broad peak identified at 3050 to 2800 cm^{-1} corresponds with stretching vibrations of a methyl group (CH3) are associated with monitoring the lipids and proteins of the sample (Korkmaz, & Severcan, 2005). Fig. 3 showed that the 3050 to 2800 cm^{-1} normalized concerning the CH3 groups' asymmetric and symmetric stretching vibrations at 2957 and 2873 cm^{-1}, respectively (Dogan, Siyakus, & Severcan, 2007). The absorbance of germinated cowpea flour cultivars also showed an increasing trend compared to native ones in the 3050 to 2800 cm^{-1} regions representing modifications in lipid and protein ratios of germinated flour. The germination increased intensities of asymmetric stretching vibrations (2957 cm^{-1}) from 0.018 to 0.021 and 0.010 to 0.024, and symmetric stretching vibrations (2873 cm^{-1}) from 0.016 to 0.018 and 0.09 to 0.022, in Black and White cowpea flour cultivars, respectively. The absorbance ratio at 2854 to 2873 cm-1 represents the change in lipid/protein ratio (Boyar, Zorlu, Mut, & Severcan, 2004). The lipid/protein ratio of germinated cowpea increased from 0.96 to 0.97 and 0.88 to 0.95 in black and white cultivars, indicating the increased intensity of CH2 symmetric stretching vibra-

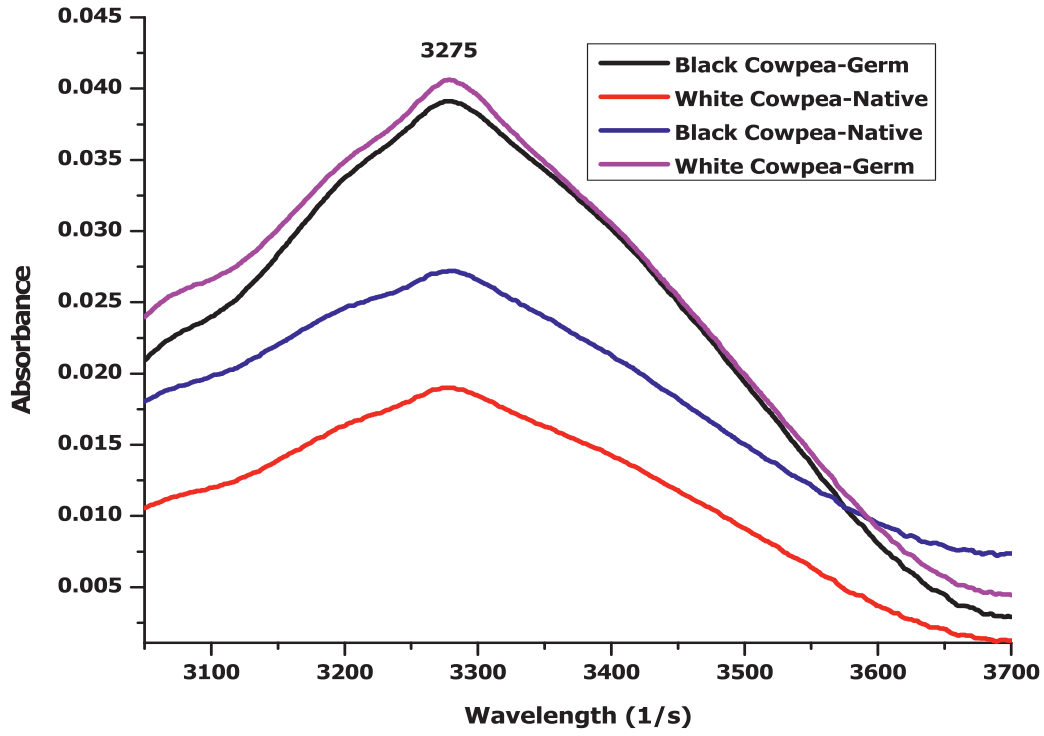

Fig. 2. Spectra of native and germinate cowpea flour cultivars in 3700-3050 cm^{-1} region normalized concerning Amide A Band at 3275 cm^{-1}.

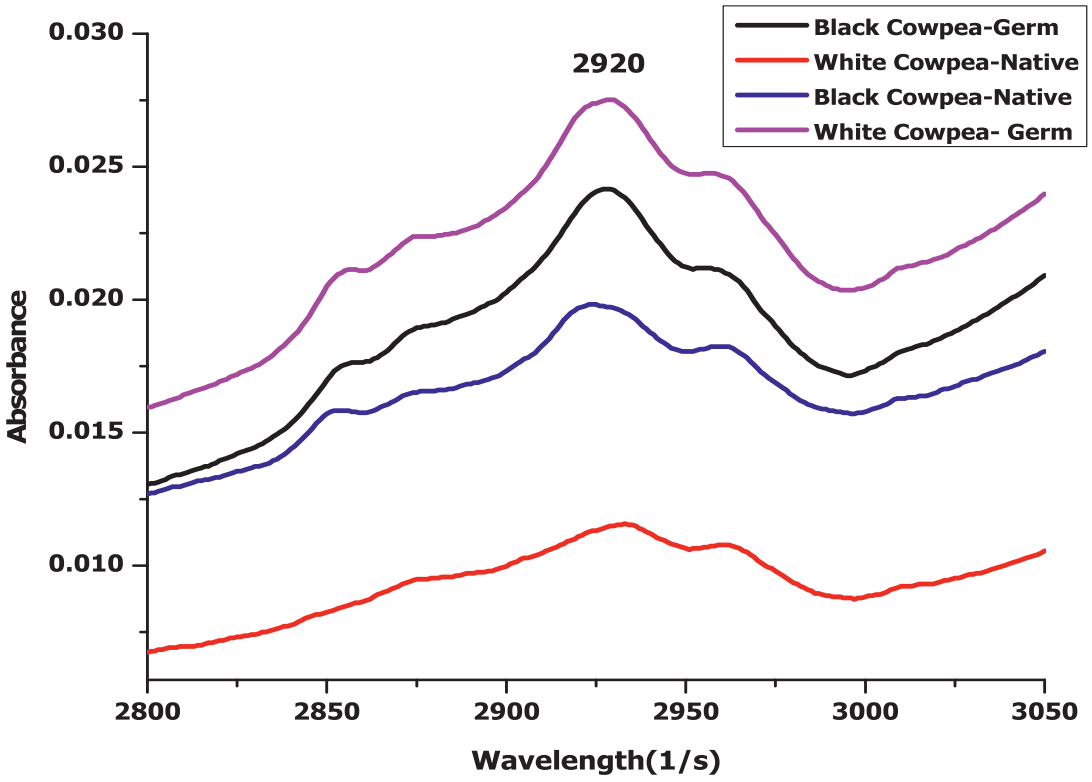

Fig. 3. Spectra of native and germinate cowpea flour cultivars in the 3050-2800 cm^{-1} region normalized concerning the CH3 asymmetric band at 2926 cm^{-1}.

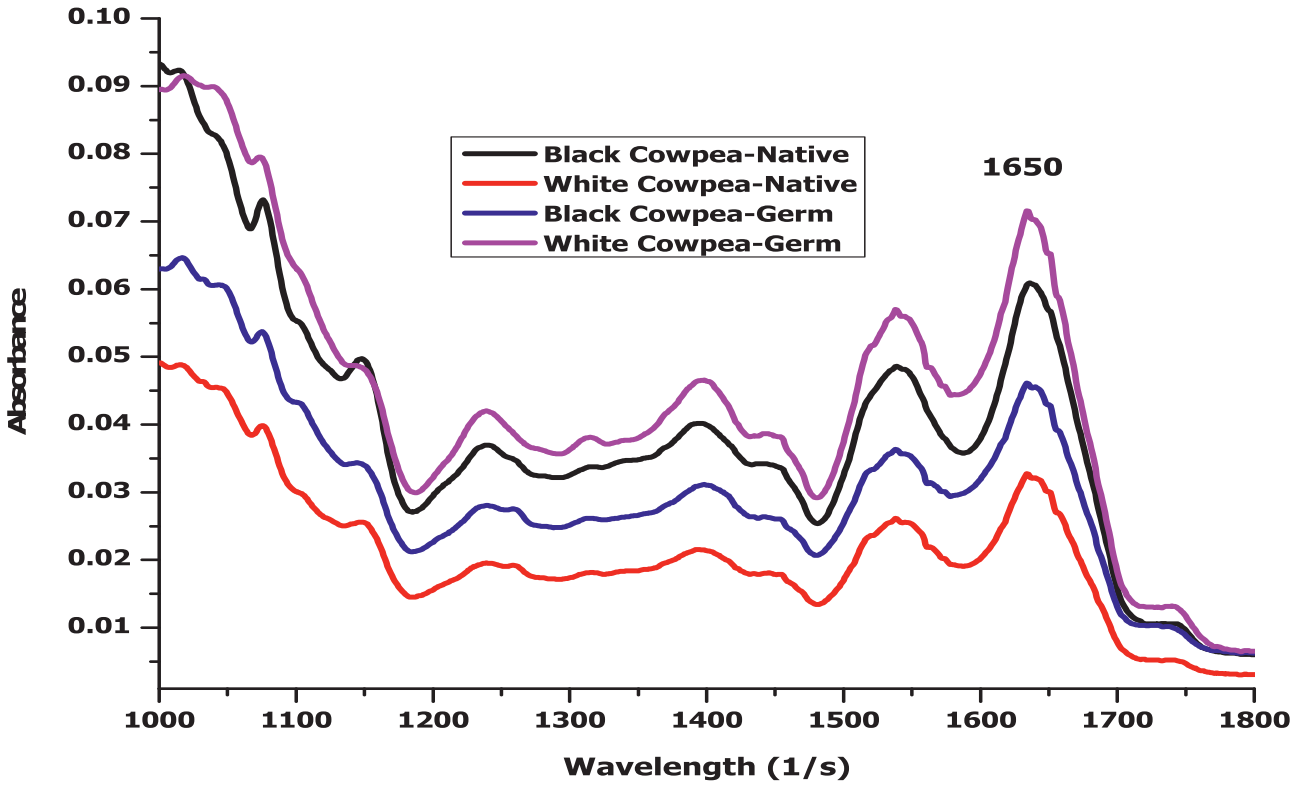

Fig. 4. Spectra of native and germinate cowpea flour cultivars in the 1800-1000cm^{-1} region normalized concerning the Amide I band at 1650 cm^{-1}.

tions. The frequency range of 1800 to 1000 cm^{-1} showed peaks around bands at 1746 cm^{-1}, 1650 cm^{-1}, and 1546 cm^{-1} related to ester C=O stretching of lipids (Gunarathne, Marikkar, Yalegama, & Mendis, 2022), Amide I and Amide II of structural proteins (Dogan, Siyakus, & Severcan, 2007). The 1800 to 1000 region of germinated cowpea flour cultivars observed an increase in absorbance compared to native (Fig. 4), revealing a change in lipid-protein ratio and secondary protein structures of cowpea flour under the germination process.

3.2. Starch short-range ordered structures of cowpea flour

The ATR FT-IR spectroscopy (800 to 1200 cm^{-1}) corresponds to a fingerprinting region associated with C–C, C–O, and C–H stretching vibrations (Siwatch, Yadav, & Yadav, 2017). The fingerprint region is associated with wavelengths of 1047, 1022, and 995 cm^{-1} to determine short-range ordered structures of starch in different starch types of food products. The band at 1047 cm^{-1} corresponds ordered structure of starch, 1022 cm^{-1} for the amorphous nature of starch, and 995 cm^{-1} for the hydrated crystalline nature of starchy substances (Capron, Robert, Colonna, Brogly, & Planchot, 2007; Bello-Perez, Ottenhof, Agama-Acevedo, & Farhat, 2005). The absorbance of specific wavenumber at 995, 1022, and 1047 cm^{-1} were 0.062, 0.063, 0.062, 0.048, 0.047 and 0.045 abs in native black and white cowpea cultivars, respectively. With germination, the absorbance of bands showed an increased trend in cowpea flour (Fig. 5). The absorbance of the 1047/1022 cm^{-1} ratio determines the ordered to amorphous starch and the 1022/995 cm^{-1} ratio for localization of double helices starch within crystallites (Wang et al., 2015). The ratio of 1047/1022 cm^{-1} was 0.952 and 0.957 in native and 0.910 and 0.967 in germinated Black and White cowpea flour, and 1022/995 cm^{-1} ratio of 1.016 and 0.979 in native and 0.967 and 1.034 in germinated Black and White cowpea flour, respectively. The 1047/1022 cm^{-1} and 1022/995 cm^{-1} absorbance ratios of wavenumber decreased in Black cowpea flour and increased in White cowpea flour due to germination. This showed alteration of the ordered structure of starch fraction of cowpea flour during germination. The 1047/1022 cm^{-1} and 1022/995 cm^{-1} ratios in Black cowpea flour under germination showed a reduction of short-range ordered structures and long-ordered starch fraction in germinated White cowpea flour. The study justfy the degree of ordered starch and their alteration in terms of amorphous/crystallinity nature concerning germination and cultivars. Therefore, the study of starch order structure is critical for understanding germinated flours' functionality and potential applications in food applications (Gutiérrez-Osnaya et al., 2020).

3.3. Protein secondary structure of cowpea flour

The secondary structure of native and germinated cowpea flour represents (Table 1) the average summative percentage areas, and Fig. 6 shows the deconvoluted Gaussian-shaped curves of the amide I band of germinated cowpea flour. The 1700-1600 cm^{-1} is the sensitive region related to Amide-I raised due to C=O stretching of the peptide group and is associated with the sum of the overlapped structures such as β-sheet, random coils, α-helix, and β-turns (Xu et al., 2020). The amide I peak frequencies of 1648-1660 cm^{-1} and 1630 cm^{-1} were assigned for α-helix, 1612-1641 cm^{-1}, 1626-1640 cm^{-1}, and 1670-1694 cm^{-1} for β-sheets, 1662-1684 for turns, and 1640-1650 for random coil secondary structures (Carbonaro, & Nucara, 2010). The mean relative proportion of protein structures were 57.72 % and 51.15%, 64.67% and 31.09 % for β-sheets, 8.45 % and 0.14 %, 7.99 % and 4.57% for α-helix, 15.24 % and 16.40 %, 16.37% and 15.22% for turns, and 14.30 % and 30.67%, 1.24 % and 19.25% for random coils of native and germinated Black and White cowpea cultivars. The β-sheets and α-helix content are related to ordered protein structures (Sofi, Singh, Muzaffar, & Dar, 2021). The β-sheets were reported highest proportions as compared to α-helix content

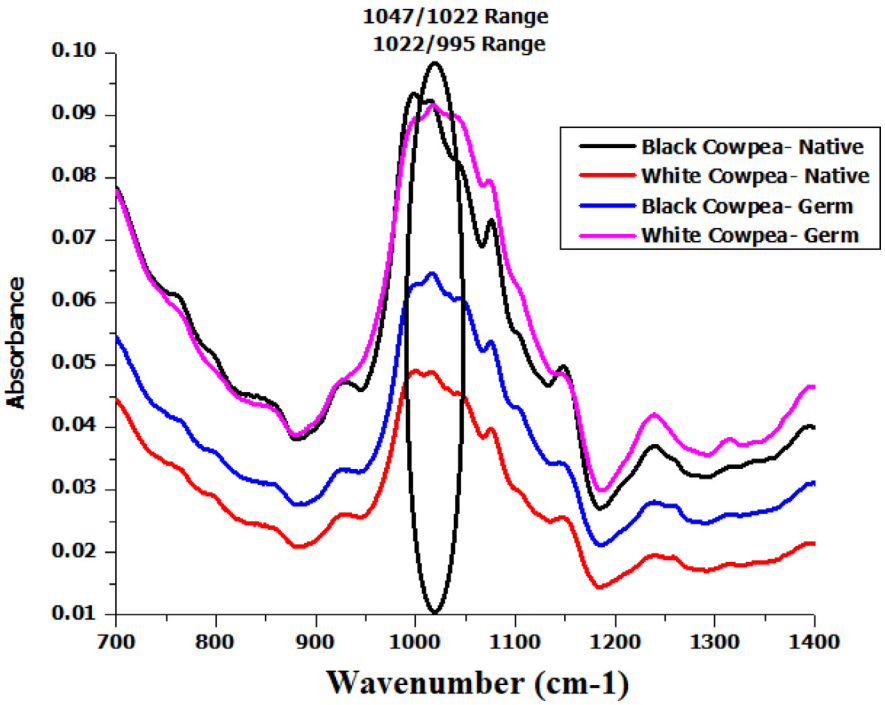

Fig. 5. Fingerprint region (1200 to 800 cm^{-1}) of native and germinate cowpea flour for ordered structures.

Table 1
The relative proportion of protein secondary structure in native and germinated cowpea flour cultivars.

Sample	B-sheets (%)	α-Helix (%)	Random Coil (%)	Turn (%)
Black Cowpea-Native	57.72 ± 0.65^{c}	8.45 ± 0.14^{d}	14.3 ± 0.08^{b}	15.24 ± 0.10^{b}
Black Cowpea-Germ	51.15 ± 0.87^{b}	0.14 ± 0.08^{a}	30.67 ± 0.04^{d}	16.40 ± 0.13^{d}
White Cowpea-Native	64.67 ± 0.62^{d}	7.99 ± 0.12^{c}	1.24 ± 0.02^{a}	15.22 ± 0.09^{a}
White Cowpea-Germ	31.09 ± 0.72^{a}	4.57 ± 0.17^{b}	19.25 ± 0.11^{c}	16.37 ± 0.08^{c}

Values were expressed as the average of triplicates ± Standard deviation
Different superscript letters (a–d) in the same column indicate a significant difference between native and germinated flour from cowpea chickpea cultivars

in cowpea cultivars, as similar results were reported in different pulses flours by Shevkani, Singh, Rana, & Kaur (2014) and Ghumman, Kaur, & Singh, (2016). The result showed a shift of β-sheets and α-helix into random coils and β-turn structures, representing an increase in germinated cowpea flour's amorphous structure compared to native. The decreased proportion of ordered structures of β-sheet and α-helix during germination breaks their hydrogen bonding and converts them into disordered structures (turns and random coils) (Xu et al., 2020).

3.4. Intrinsic fluorescence spectroscopy

Intrinsic fluorescence is related to characterizing the tertiary structure of the proteins by determining the behavior of fluorescent compounds on the molecular surface of proteins (Chen, Chen, Ren, & Zhao, 2011). The fluorescent compounds (tryptophan, tyrosine and phenylalanine) altered under the fluorescence spectrum reflects the change in protein conformational structure at the tertiary level (Shen, & Tang, 2012). The maximum absorption concerning the fluorescence peak emission of proteins shifted to the right (red shift) and left (blue shift) represents the degree of protein conformations (Wang et al., 2020). The germinated flours shifts in the maximum fluorescence intensity (347 to 348 nm), reflecting the redshifts in germinated flours due to the protein unfolding chain and hence increased concentrations of fluorescent compounds in the medium (Kristo, Hazizaj, & Corredig, 2012). Fig. 7 showed maximum fluorescence intensities in native flours compared to germinated ones, reflecting the decreased concentrations of fluorescent compounds during germination in cowpea flour. The decreased fluorescence emission spectrum of germinated cowpea was due to alteration in the protein chain by activation of endogenous enzymes during germination, resulting in exposure of fluorescent compounds in an aqueous medium (Kang, Zhang, Guo, Lei, & Yang, 2022).

3.5. Ultraviolet spectrum analysis

Ultraviolet spectrum was used in the cowpea flour samples to analyze the change in protein conformation. The cowpea flour under germination treatment alters the nutrients such as proteins which contain side chains residues of tryptophan, tyrosine, phenylalanine, histidine, and cysteine amino acids that produce ultraviolet absorption spectrum (Kelly, Jess, & Price, 2005). Fig. 8 shows the ultraviolet spectrum with an almost similar spectrum in native and germinated cowpea flour. The maximum absorption at 210 nm was reported in all the flour samples. The maximum absorption peak in the ultraviolet absorption spectrum of cowpea flour samples was observed towards the short wave direc-

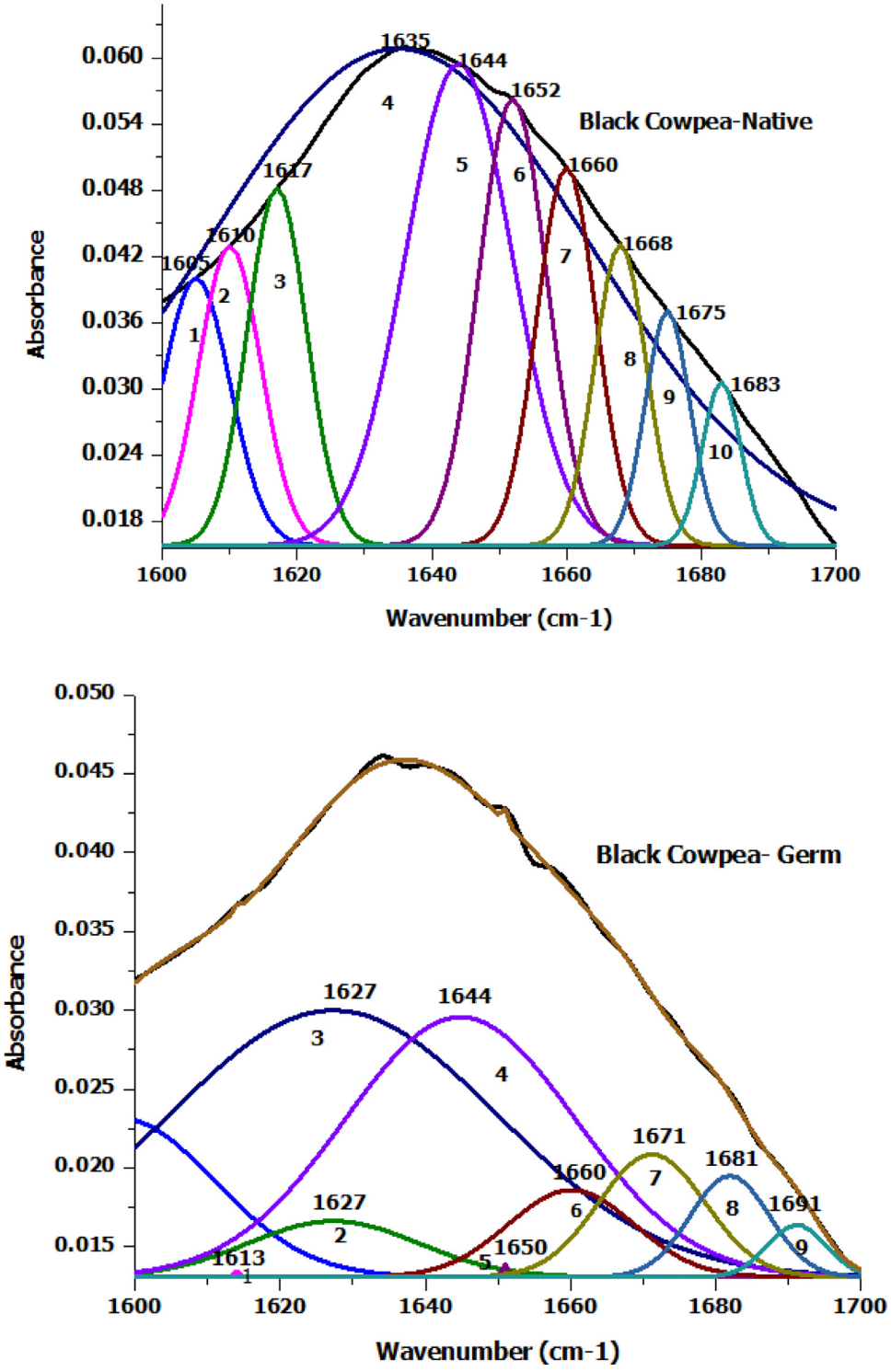

Fig. 6. De-convoluted amide I bands of protein secondary structure of native and germinate cowpea flour cultivars.

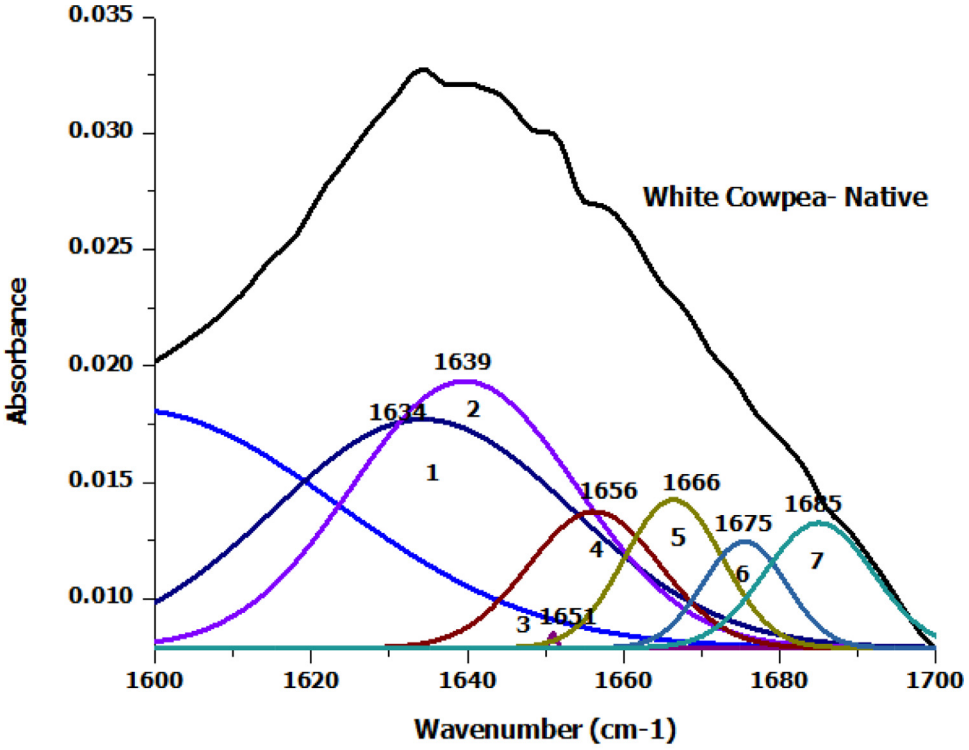

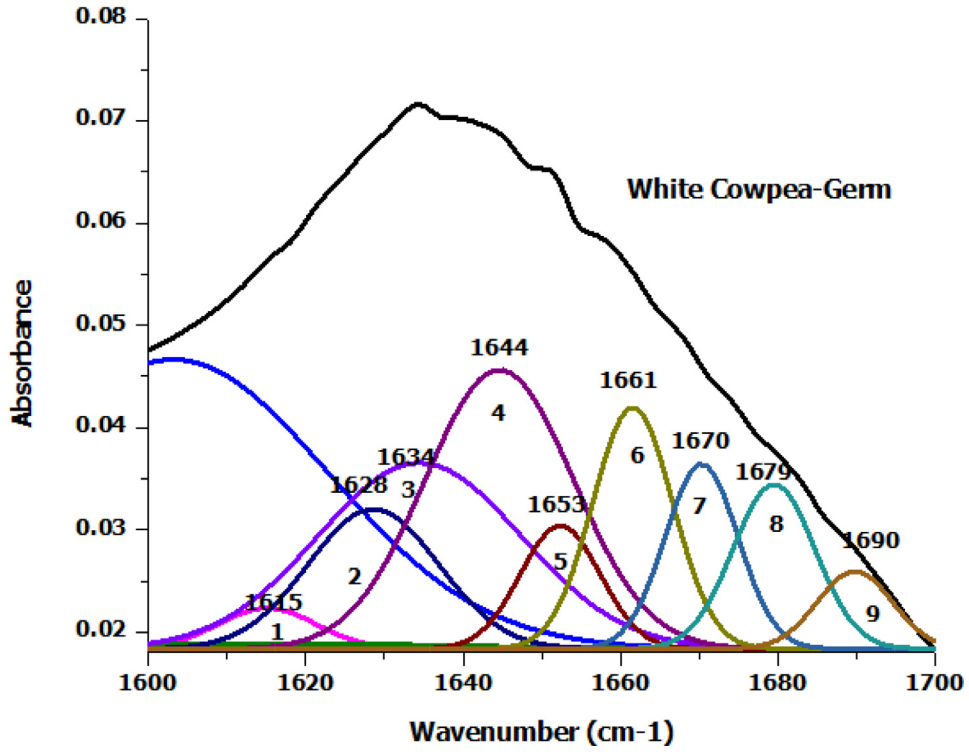

Fig. 6. Continued

tion resulting in the spectrum shifting towards a blue shift (Wang et al., 2020). The blue shift of flours could be related to the protein modification under germination that alters the protein structure that increases the absorption of ultraviolet light by tryptophan tyrosine and phenylalanine residue, and a blue shift occurred.

3.6. Sodium dodecyl sulphate polyacrylamide gel electrophoresis (SDS-PAGE)

SDS-PAGE of native and germinated black and white cowpea cultivars are presented in Fig. 9, and quantitative data of band with relative

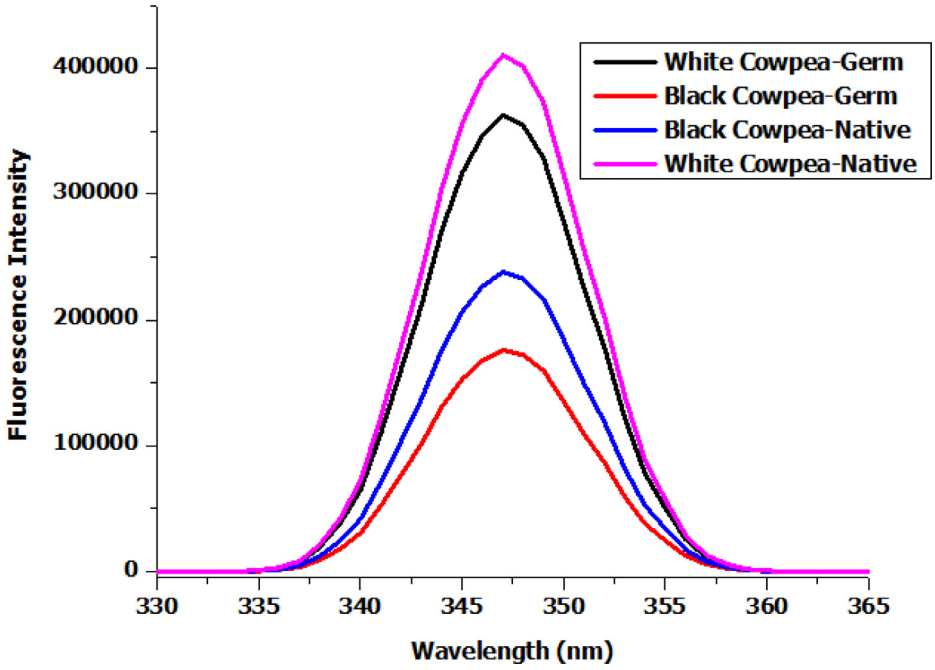

Fig. 7. Intrinsic fluorescence analysis of native and germinate cowpea flour cultivars.

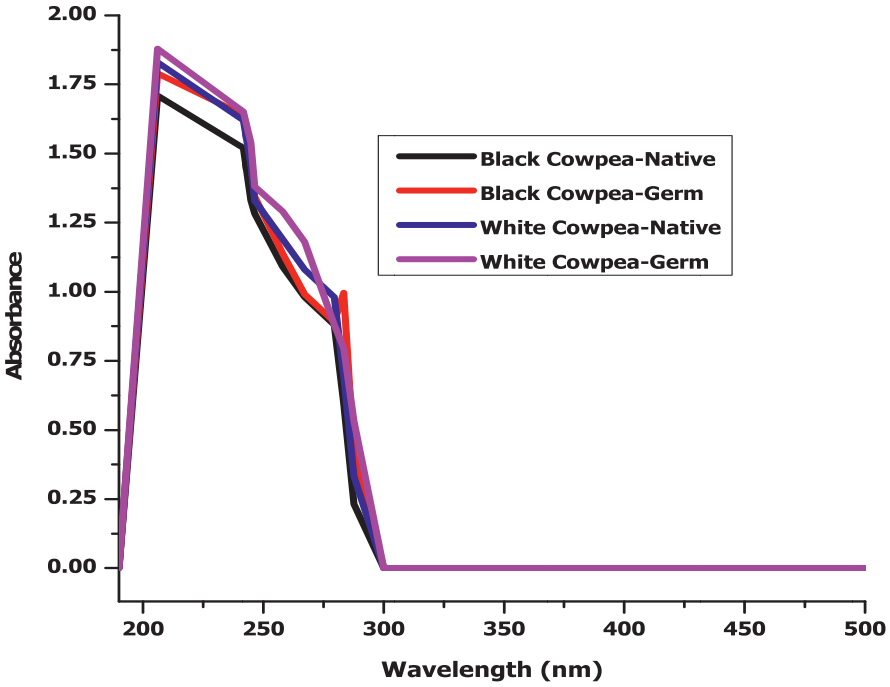

Fig. 8. UV Spectrum analysis of native and germinate cowpea flour cultivars.

migration (Rf) are in Table 2. The protein profiling of the electropherogram showed a range of molecular weights from 10 to 225 kDa. The White and Black cowpea native showed bands at 214.50, 102.88, 86.19, 77.84, 60.20, 44.03, 32.12, 28.59, 23.32, 18.39, 13.16 and 8.99 kDa and 207.05, 143.79, 116.62, 105.97, 82.25, 63.51, 53.96, 44.10, 31.43, 24.65, 21.99 17.75, 12.55, 10.15 and 8.17 kDa. The bands showed increase in protein bands upon germination at 206.73, 112.73, 103.42, 87.89, 77.50, 59.24, 43.21, 28.70, 23.33, 18.41, 16.73, 12.97 and 8.81 kDa in White cowpea germ, and 149.69, 123.25, 114.92, 102.53, 88.45, 68.96, 57.82, 48.98, 41.60, 27.13, 22.27, 19.27, 17.14, 13.58, 11.06 and 8.74 kDa in Black cowpea germ. The variations in the intensities of high (25 to 225 kDa) and low (19 to 10 kDa) molecular weight proteins in

Table 2
The relative proportion of center peaks, amplitude, half width and their protein secondary structure in native and germinated cowpea flour cultivars.

Black Cowpea Native					Black Cowpea Germ				
Peak No.	Centre Peak	Amplitude	Half Width	Structure	Peak No.	Centre Peak	Amplitude	Half Width	Structure
1	1605	0.02426	11.83002	B-sheets	1	1613	0.0101	0.0006	B-sheets
2	1610	0.02713	10.92694	B-sheets	2	1627	0.0004	27.53	B-sheets
3	1617	0.03239	10.37172	B-sheets	3	1627	0.0035	53.51	B-sheets
4	1635	0.04504	66.99493	B-sheets	4	1644	0.0169	37.46	Random Coils
5	1644	0.0437	18.6079	Random Coils	5	1650	0.016	0.046	α-Helix
6	1652	0.04052	11.86405	α-Helix	6	1660	0.0008	20.37	Turn
7	1660	0.03429	10.3478	Turn	7	1671	0.005	17.3	B-sheets
8	1668	0.02728	9.03823	Turn	8	1681	0.007	12.83	B-sheets
9	1675	0.02127	7.81196	B-sheets	9	1691	0.006	9.5	B-sheets
10	1683	0.01484	6.7174	B-sheets					
White Cowpea Native					**White Cowpea Germ**				
Peak No.	Centre Peak	Amplitude	Half Width	Structure	Peak No.	Centre Peak	Amplitude	Half Width	Structure
1	1634	0.0098	45.05	B-sheets	1	1615	0.004	54.17	B-sheets
2	1639	0.011	33.86	B-sheets	2	1628	0.013	19.49	B-sheets
3	1656	0.0058	19.82	α-Helix	3	1634	0.018	30.41	B-sheets
4	1666	0.0063	14.79	Turn	4	1644	0.027	22.21	Random Coils
5	1651	0.00077	0.050	Random Coils	5	1653	0.012	11.96	α-Helix
6	1675	0.0045	12.54	B-sheets	6	1661	0.023	11.92	Turn
7	1685	0.0053	16.28	B-sheets	7	1670	0.018	10.90	B-sheets
					8	1679	0.016	12.22	B-sheets
					9	1690	0.007	11.16	B-sheets

Table 3
Quantitative analysis of SDS-PAGE of analysis of native and germinate cowpea flour cultivars.

White Cowpea –Native (1)			White Cowpea –Germ (2)			Black Cowpea –Native (3)			Black Cowpea –Germ (4)		
Band No.	Relative Migration (Rf)	Molecular weight (KDa)	Band No.	Relative Migration (Rf)	Molecular weight (KDa)	Band No.	Relative Migration (Rf)	Molecular weight (KDa)	Band No.	Relative Migration (Rf)	Molecular weight (KDa)
1	0.041	214.50	1	0.052	206.73	1	0.052	207.05	1	0.146	149.69
2	0.256	102.88	2	0.229	112.73	2	0.158	143.79	2	0.203	123.25
3	0.307	86.19	3	0.254	103.42	3	0.219	116.62	3	0.223	114.92
4	0.337	77.84	4	0.302	87.89	4	0.247	105.97	4	0.257	102.53
5	0.412	60.20	5	0.338	77.50	5	0.321	82.25	5	0.300	88.45
6	0.503	44.03	6	0.417	59.24	6	0.397	63.51	6	0.372	68.96
7	0.595	32.12	7	0.509	43.21	7	0.444	53.96	7	0.424	57.82
8	0.629	28.59	8	0.628	28.70	8	0.503	44.10	8	0.472	48.98
9	0.689	23.32	9	0.689	23.33	9	0.602	31.43	9	0.520	41.60
10	0.758	18.39	10	0.758	18.41	10	0.673	24.65	10	0.645	27.13
11	0.856	13.16	11	0.786	16.73	11	0.706	21.99	11	0.702	22.27
12	0.967	8.99	12	0.860	12.97	12	0.769	17.75	12	0.745	19.27
-	-	-	13	0.973	8.81	13	0.870	12.55	13	0.779	17.14
-	-	-	-	-	-	14	0.932	10.15	14	0.847	13.58
-	-	-	-	-	-	15	0.995	8.17	15	0.907	11.06
-	-		-	-	-	-	-	-	16	0.975	8.74

germinated cowpea cultivars than the native one. The change in intensity may be related to activated proteolytic enzymes during germination (Ghumman, Kaur, & Singh, 2016). The SDS Page showed variations in white and black cowpea cultivars, which is related to their difference in their protein profiling and spectroscopic properties between the cowpea cultivars Table 3.

4. Conclusions

The germination process is a low cost technology associated with metabolic activities in the grain, which results in improving the nutritional profile and alternations of biochemical constituents. The cowpea a rich source of proteins with wide industrial application for development of functional foods like sprouts, fermented flour, gluten free products, peptides, canned products and vegan foods. Spectroscopic techniques are used to reveal the change in chemical constituents in pulses under germination. The ATIR-FTIR showed alterations in protein structures and starch crystallinity of germinated cowpea cultivars. Intrinsic fluorescence showed decreasing fluorescence, and UV spectrum revealed an increase in maximum absorption, indicating biochemical modification in cowpea flour under germination. The electrophoresis also showed a change in protein intensities in germinated cowpea cultivars. The spectroscopy technique can be one of the methods to reveal the modifications in the germinated grains at industrial level. Future prospects and commercial importance of the study will be spectroscopic methods for quantitative analysis, characterization and quality control in pulse research and pulse based functional food products.

Ethical statement

No animal or human subjects were used in this study.

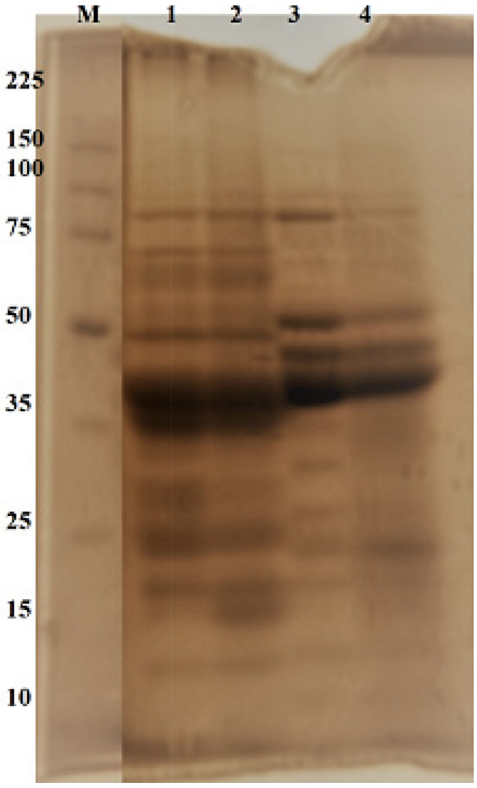

Fig. 9. Electrophoresis of analysis of native and germinate cowpea flour cultivars.

Declaration of Competing Interest

The authors declare no conflict of interest.

CRediT authorship contribution statement

Sajad Ahmad Sofi: Conceptualization, Methodology, Software, Investigation, Resources, Data curation, Writing – original draft, Project administration, Validation. **Khalid Muzaffar:** Writing – review & editing, Visualization. **Asmat Farooq:** Resources, Writing – original draft. **Shafiya Rafiq:** Resources, Data curation, Writing – review & editing, Visualization. **Darakshan Majid:** Writing – review & editing, Visualization. **Hilal Ahmad Makroo:** Supervision, Visualization, Writing – review & editing. **Shabir Ahmad Mir:** Writing – review & editing, Visualization. **Amin Mousavi Khaneghah:** Resources, Data curation, Writing – review & editing, Visualization. **Francisco J. Barba:** Supervision, Visualization, Writing – review & editing. **B.N. Dar:** Supervision, Project administration, Validation, Investigation.

Data Availability

The authors do not have permission to share data.

References

Adjei-Fremah, S., Worku, M., De Erive, M. O., He, F., Wang, T., & Chen, G. (2019). Effect of microfluidization on microstructure, protein profile and physicochemical properties of whole cowpea flours. *Innovative Food Science & Emerging Technologies, 57*, Article 102207.

Appiah, F., Asibuo, J. Y., & Kumah, P. (2011). Physicochemical and functional properties of bean flours of three cowpea (*Vigna unguiculata* L. Walp) varieties in Ghana. *Journal of Food Science, 5*(2), 100–104.

Barron, C., Parker, M. L., Mills, E. N. C., Rouau, X., & Wilson, R. H. (2005). FTIR imaging of wheat endosperm cell walls *in situ* reveals compositional and architectural heterogeneity related to grain hardness. *Planta, 220*(5), 667–677.

Bello-Perez, L. A., Ottenhof, M. A., Agama-Acevedo, E., & Farhat, I. A. (2005). Effect of storage time on the retrogradation of banana starch extrudate. *Journal of Agricultural and Food Chemistry, 53*(4), 1081–1086.

Boyar, H., Zorlu, F., Mut, M., & Severcan, F. (2004). The effects of chronic hypoperfusion on rat cranial bone mineral and organic matrix. *Analytical and Bioanalytical chemistry, 379*(3), 433–438.

Capron, I., Robert, P., Colonna, P., Brogly, M., & Planchot, V. (2007). Starch in rubbery and glassy states by FTIR spectroscopy. *Carbohydrate Polymer, 68*(2), 249–259.

Carbonaro, M., & Nucara, A. (2007). Application of FT-IR spectroscopy in the assessment of changes in the secondary structure of food proteins taking legumes as a model. *Amino Acids, 33*, 45–46.

Carbonaro, M., & Nucara, A. (2010). Secondary structure of food proteins by Fourier transform spectroscopy in the mid-infrared region. *Amino Acids, 38*(3), 679–690.

Carbonaro, M., Maselli, P., Dore, P., & Nucara, A. (2008). Application of Fourier transform infrared spectroscopy to legume seed flour analysis. *Food Chemistry, 108*(1), 361–368.

Chávez-Murillo, C. E., Veyna-Torres, J. I., Cavazos-Tamez, L. M., de la Rosa-Millán, J., & Serna-Saldívar, S. O. (2018). Physicochemical characteristics, ATR-FTIR molecular interactions and *in vitro* starch and protein digestion of thermally-treated whole pulse flours. *Food Research International, 105*, 371–383.

Chen, L., Chen, J., Ren, J., & Zhao, M. (2011). Effects of ultrasound pretreatment on the enzymatic hydrolysis of soy protein isolates and on the emulsifying properties of hydrolysates. *Journal of Agricultural & Food Chemistry, 59*(6), 2600–2609.

Cocchi, M., Foca, G., Lucisano, M., Marchetti, A., Pagani, M. A., Tassi, L., & Ulrici, A. (2004). Classification of cereal flours by chemometric analysis of MIR spectra. *Journal of Agricultural and Food Chemistry, 52*(5), 1062–1067.

De la Rosa-Millán, J., Orona-Padilla, J. L., Flores-Moreno, V. M., & Serna-Saldívar, S. O. (2018). Physicochemical, functional and ATR-FTIR molecular analysis of protein extracts derived from starchy pulses. *International Journal of Food Science & Technology, 53*(6), 1414–1424.

De Souza Rocha, T., Hernandez, L. M. R., Chang, Y. K., & de Mejía, E. G. (2014). Impact of germination and enzymatic hydrolysis of cowpea bean (Vigna unguiculata) on the generation of peptides capable of inhibiting dipeptidyl peptidase IV. *Food Research International, 64*, 799–809.

Doblado, R., Frías, J., & Vidal-Valverde, C. (2007). Changes in vitamin C content and antioxidant capacity of raw and germinated cowpea (Vigna sinensis var. carilla) seeds induced by high pressure treatment. *Food Chemistry, 101*(3), 918–923.

Dogan, A., Siyakus, G., & Severcan, F. (2007). FTIR spectroscopic characterization of irradiated hazelnut (Corylus avellana L.). *Food Chemistry, 100*(3), 1106–1114.

Domínguez-Arispuro, D. M., Cuevas-Rodríguez, E. O., Milán-Carrillo, J., León-López, L., Gutiérrez-Dorado, R., & Reyes-Moreno, C. (2018). Optimal germination condition impacts on the antioxidant activity and phenolic acids profile in pigmented desi chickpea (Cicer arietinum L.) seeds. *Journal of Food Science and Technology, 55*(2), 638–647.

Ferreira, D. S., Pallone, J. A. L., & Poppi, R. J. (2015). Direct analysis of the main chemical constituents in Chenopodium quinoa grain using Fourier transform near-infrared spectroscopy. *Food Control, 48*, 91–95.

Ferreira, D., Barros, A., Coimbra, M. A., & Delgadillo, I. (2001). Use of FT-IR spectroscopy to follow the effect of processing in cell wall polysaccharide extracts of a sun-dried pear. *Carbohydrate Polymers, 45*(2), 175–182.

Ghumman, A., Kaur, A., & Singh, N. (2016). Impact of germination on flour, protein and starch characteristics of lentil (*Lens culinary* L.) and horse gram (*Macrotyloma uniflorum* L.) lines. *LWT- Food Science & Technology, 65*, 137–144.

Gunarathne, R., Marikkar, N., Yalegama, C., & Mendis, E. (2022). FTIR spectral analysis combined with chemometrics in evaluation of composite mixtures of coconut testa flour and wheat flour. *Journal of Food Measurement and Characterization, 16*(3), 1796–1806.

Gutiérrez-Osnaya, L. J., Hernández-Uribe, J. P., Castro-Rosas, J., Román-Gutiérrez, A. D., Camacho-Díaz, B. H., Palma-Rodríguez, H. M., & Guzmán-Ortiz, F. A. (2020). Influence of germination time on the morphological, morphometric, structural, and physicochemical characteristics of Esmeralda and Perla barley starch. *International Journal of Biological. Macromolecules, 149*, 262–270.

Hell, J., Prückler, M., Danner, L., Henniges, U., Apprich, S., Rosenau, T., & Böhmdorfer, S. (2016). A comparison between near-infrared (NIR) and mid-infrared (ATR-FTIR) spectroscopy for the multivariate determination of compositional properties in wheat bran samples. *Food Control, 60*, 365–369.

Holse, M., Larsen, F. H., Hansen, Å., & Engelsen, S. B. (2011). Characterization of marama bean (*Tylosema esculentum*) by comparative spectroscopy: NMR, FT-Raman, FT-IR and NIR. *Food Research International, 44*(1), 373–384.

Horn, L. N., & Shimelis, H. (2020). Production constraints and breeding approaches for cowpea improvement for drought prone agro-ecologies in Sub-Saharan Africa. *Annals of Agricultural Sciences, 65*(1), 83–91.

Hou, Y., Zhao, P., Zhang, F., Yang, S., Rady, A., Wijewardane, N. K., & Li, M. (2022). Fourier-transform infrared spectroscopy and machine learning to predict amino acid content of nine commercial insects. *Food Science and Technology, 42*, 1590.

Jayathilake, C., Visvanathan, R., Deen, A., Bangamuwage, R., Jayawardana, B. C., Nammi, S., & Liyanage, R. (2018). Cowpea: An overview on its nutritional facts and health benefits. *Journal of the Science of Food and Agriculture, 98*(13), 4793–4806.

Kang, S., Zhang, J., Guo, X., Lei, Y., & Yang, M. (2022). Effects of ultrasonic treatment on the structure, functional properties of chickpea protein isolate and its digestibility *in vitro*. *Foods, 11*(6), 880.

Kelly, S. M., Jess, T. J., & Price, N. C. (2005). How to study proteins by circular dichroism. *Biochimica et Biophysica Acta (BBA)-Proteins and Proteomics, 1751*(2), 119–139.

Kong, J., & Yu, S. (2007). Fourier transform infrared spectroscopic analysis of protein secondary structures. *Acta Biochimica et Biophysica Sinica, 39*(8), 549–559.

Korkmaz, F., & Severcan, F. (2005). Effect of progesterone on DPPC membrane: Evidence for lateral phase separation and inverse action in lipid dynamics. *Archives of Biochemistry and Biophysics, 440*(2), 141–147.

Kristo, E., Hazizaj, A., & Corredig, M. (2012). Structural changes imposed on whey proteins by UV irradiation in a continuous UV light reactor. *Journal of Agricultural & Food Chemistry, 60*(24), 6204–6209.

Laemmli, U. K. (1970). Cleavage of structural proteins during the assembly of bacteriophage T4. *Nature, 227*, 680–685.

Lenhardt, L., Bro, R., Zeković, I., Dramićanin, T., & Dramićanin, M. D. (2015). Fluorescence spectroscopy coupled with PARAFAC and PLS DA for characterization and classification of honey. *Food Chemistry, 175*, 284–291.

Madodé, Y. E., Nout, M. J., Bakker, E. J., Linnemann, A. R., Hounhouigan, D. J., & van Boekel, M. A. (2013). Enhancing the digestibility of cowpea (*Vigna unguiculata*) by traditional processing and fermentation. *LWT-Food Science and Technology, 54*(1), 186–193.

Medhe, S. V., Kamble, M. T., Kettawan, A. K., Monboonpitak, N., & Kettawan, A. (2022). Effect of hydrothermal cooking and germination treatment on functional and physicochemical properties of parkia timoriana bean flours: An underexplored legume species of Parkia genera. *Foods, 11*(13), 1822.

Mir, S. A., Farooq, S., Shah, M. A., Sofi, S. A., Dar, B. N., Hamdani, A. M., & Khaneghah, A. M. (2021). An overview of sprouts nutritional properties, pathogens and decontamination technologies. *LWT-Food Science and Technology, 141*(2021), Article 110900.

Ouazib, M., Dura, A., Zaidi, F., & Rosell, C. M. (2016). Effect of partial substitution of wheat flour by processed (germinated, toasted, cooked) chickpea on bread quality. *International Journal of Agricultral Science & Technology, 4*(1), 2327–7246.

Prates, L. L., Lei, Y., Refat, B., Zhang, W., & Yu, P. (2018). Effects of heat processing methods on protein subfractions and protein degradation kinetics in dairy cattle in relation to protein molecular structure of barley grain using advanced molecular spectroscopy. *Journal of Cereal Science, 80*, 212–220.

Preethi, R., Moses, J. A., & Anandharamakrishnan, C. (2021). Effect of conductive hydro-drying on physiochemical and functional properties of two pulse protein extracts: Green gram (Vigna radiata) and black gram (Vigna mungo). *Food Chemistry, 343*, Article 128551.

Sevenou, O., Hill, S. E., Farhat, I. A., & Mitchell, J. R. (2002). Organisation of the external region of the starch granule as determined by infrared spectroscopy. *International Journal of Biological Macromolecules, 31*(1-3), 79–85.

Shen, L., & Tang, C. H. (2012). Microfluidization as a potential technique to modify surface properties of the soy protein isolate. *Food Research International, 48*(1), 108–118.

Shevkani, K., Singh, N., Chen, Y., Kaur, A., & Yu, L. (2019). Pulse proteins: Secondary structure, functionality and applications. *Journal of food science and technology, 56*(6), 2787–2798.

Shevkani, K., Singh, N., Rana, J. C., & Kaur, A. (2014). Relationship between physicochemical and functional properties of amaranth (*Amaranthus hypochondriacus*) protein isolates. *International Journal Food Science & Technology, 49*(2), 541–550.

Siwatch, M., Yadav, R. B., & Yadav, B. S. (2017). X-ray diffraction, rheological and FT-IR spectra studies of processed amaranth (*Amaranthus hypochondriacus*). *Journal of Food Measurement & Characterization, 11*(4), 1717–1724.

Sofi, S. A., Singh, J., Muzaffar, K., & Dar, B. N. (2021). Effect of germination time on physicochemical, electrophoretic, rheological, and functional performance of chickpea protein isolates. *ACS Food Science & Technology, 1*(5), 802–812.

Vatansever, S., Ohm, J. B., Simsek, S., & Hall, C. (2022). A novel approach: Supercritical carbon dioxide+ ethanol extraction to improve techno-functionalities of pea protein isolate. *Cereal Chemistry, 99*(1), 130–143.

Wang, S., Sun, Y., Wang, J., Wang, S., & Copeland, L. (2016). Molecular disassembly of rice and lotus starches during thermal processing and its effect on starch digestibility. *Food & Function, 7*(2), 1188–1195.

Wang, S., Wang, J., Zhang, W., Li, C., Yu, J., & Wang, S. (2015). Molecular order and functional properties of starches from three waxy wheat varieties grown in China. *Food Chemistry, 181*, 43–50.

Wang, Y., Zhang, A., Wang, Y., Wang, X., Xu, N., & Jiang, L. (2020). Effects of irradiation on the structure and properties of glycosylated soybean proteins. *Food & Function, 11*(2), 1635–1646.

Xu, Y., Galanopoulos, M., Sismour, E., Ren, S., Mersha, Z., Lynch, P., & Almutaimi, A. (2020). Effect of enzymatic hydrolysis using endo-and exo-proteases on secondary structure, functional, and antioxidant properties of chickpea protein hydrolysates. *Journal of Food Measurement & Characterization, 14*(1), 343–352.

Zhou, F. Y., Liang, J., Kuang, H. X., & Xia, Y. G. (2022). A nondestructive solution to quantify monosaccharides by ATR-FTIR and multivariate regressions: A case study of Atractylodes polysaccharides. *Spectrochimica Acta Part A: Molecular and Biomolecular Spectroscopy*, Article 121411.

Zhu, K., Aykas, D. P., Anderson, N., Ball, C., Plans, M., & Rodriguez-Saona, L. (2022). Nutritional quality screening of oat groats by vibrational spectroscopy using field–portable instruments. *Journal of Cereal Science, 107*, Article 103520.